INTERNATIONAL JOURNAL FOR NUMERICAL METHODS IN ENGINEERING, VOL. 34, 39–59 (1992)

SHELL THEORY VERSUS DEGENERATION—A COMPARISON IN LARGE ROTATION FINITE ELEMENT ANALYSIS

NORBERT BUECHTER AND EKKEHARD RAMM

Institut fuer Baustatik, University of Stuttgart, Germany

SUMMARY

The first part of this study addresses the controversy 'degenerated solid approach' versus 'shell theory'. It is shown that both formulations differ only in the kind of discretization if they are based on the same mechanical assumptions. In particular for degenerated shell elements different versions of explicit integration across the thickness are discussed. Among these are the approximation 'Jacobian across the thickness is constant', proven to be too restrictive, and the series expansion of the inverse Jacobian which turns out to be unnecessary although it leads to equations of the same order as those of a 'best first approximation' of a shell theory.

The second part deals with the description of large rotations. It is demonstrated for problems formulated in three components of a rotation vector that a straightforward derivation results in a symmetric tangent stiffness matrix. However, a modified version is also added leading to an unsymmetric matrix already discussed in the literature. For shell problems with only two rotational variables both formulations coincide.

1. INTRODUCTION

1.1. Motivation

The derivation of shell theories has been one of the most prominent challenges in solid mechanics for many years. The considerable sophistication involved in a general shell formulation slowed down the development of efficient numerical models, at least at the beginning. Therefore, it is obvious that due to its simplicity the degenerated solid approach introduced in 1968 by Ahmad *et al.*,[1,2] in which the shell finite element is directly derived from the 3D-continuum, has been preferred by the majority of analysts. The controversy about the most preferable approach seems to be a religious war up to the present day. On one side it has been argued that shell theory is an obsolete academic exercise; one also has pointed out the difficulties of representing the rigid body modes in shell finite element formulations. Shell theoreticians in turn claimed that 'the wheel was invented a second time' and that the mechanical behaviour is rather obscured by the so-called degeneration process. In addition, they falsely blamed this approach for the existence of locking phenomena, which is rather a consequence of inconsistent interpolations than a defect of the fundamental approach. Although in the first instance both ways look very different, it is felt that they have come very close to each other in the meantime. This is mainly due to the fact that both routes have approached each other in the last years.

The fundamental equations of a non-linear shell theory including arbitrarily large rotations are known and theoretically well established. Of course the notion 'shell theory' is by far not unique.

0029–5981/92/050039–21$10.50

Received 6 December 1990
Revised 19 August 1991

The theory chosen depends on the respective mechanical assumptions. Here we like to refer to a 5-parameter theory with a Reissner–Mindlin kinematic, for example References 3, 5, 14 and 20, which may be used as a starting point for any discretization, for instance the finite element method. Typical but not absolutely necessary is the exact analytical definition of the initial geometry and the representation of the stress and strain state in curvilinear convective co-ordinates.

The degenerated solid approach discretizes the fundamental equations of the 3D-continuum introducing simultaneously physical assumptions at discrete points, usually applied in shell theory; originally also the integration across the thickness is done numerically, e.g. References 1 and 17. Typical of this approach is the isoparametric interpolation and—although the normalized element co-ordinates represent already curvilinear convective co-ordinates—stresses and strains are analysed in a local or global orthogonal Cartesian co-ordinate system, thus following the continuum-like approach. Recently, curvilinear, convective co-ordinates have also been used, e.g. for the so-called assumed strain elements.[25]

The numerical integration across the thickness following the continuum approach turned out to be extremely expensive, in particular for materials with non-constant properties in the thickness direction, e.g. for material non-linearities. Therefore, it has been proposed already in 1971[28] to explicitly integrate across the thickness introducing the classical concept of stress resultants. The related assumption of a constant Jacobian across the thickness has been proven to be too restrictive and led to considerable defects for rigid body modes of curved elements because certain terms in the definition of bending strains are missing. Presumably, this caused B. Irons in 1973 to subsequently introduce on an intuitive basis the missing terms.[11] Later on many other authors followed.

The second aspect discussed in the present study is concerned with the large rotation formulation for shells. Based on purely geometrical considerations the subject has been completely described in 1976 in References 16 and 17 essentially starting from the direction cosines of the deformed shell director. Other rotational variables have been introduced, e.g. using the rotational vector, see Section 3. Recently, the question of symmetry of the tangent operator (stiffness matrix) has been discussed, primarily when three independent rotational degrees of freedom are present as in 3D-beam analysis.[10,19,24]

1.2. Scope of study

It is one aspect of the present study to compare the concept of degeneration with a shell theory formulation for arbitrarily large rotations including transverse shear deformations. In particular, different versions of explicit integrations are discussed. In order to make the differences and identities of the two approaches transparent a notation independent of a specific co-ordinate system has been utilized; thus transformations between global and local Cartesian and curvilinear co-ordinates are avoided at this stage of the derivation. In addition, the discretization is not yet introduced at the beginning as it is usually done during the degeneration. For the sake of simplicity only a slight change of the shell thickness is allowed, i.e. the thickness is assumed to be constant.

The second part addresses the large rotation formulation. Firstly, a brief review of different options for the rotational variables is given. Secondly, the tangent operator for the rotational part is derived; the corresponding formulation is described which—although different—leads to the symmetric and unsymmetric tangent operators identical to those published in References 10, 19 and 24.

2. COMPARISON OF SHELL THEORY AND DEGENERATION

2.1. *Fundamental equations*

2.1.1. Shell theory. Here we restrict the derivation to a material formulation in the (total) Lagrangian way. The starting point is the equations of a 3D-continuum:

- Weak form of the equilibrium equation (principle of virtual work):

$$\iiint_V \mathbf{S} \cdot \delta \mathbf{E} \, \mathrm{d}V = \delta W^{\mathrm{ext}} \tag{1}$$

- kinematic equation:

$$\mathbf{F} = \frac{\partial \bar{\mathbf{x}}}{\partial \mathbf{x}} = \bar{\mathbf{x}}_{,\mathrm{x}} = \mathbf{I} + \mathbf{u}_{,\mathrm{x}} \tag{2}$$

$$\mathbf{E} = \frac{1}{2}(\mathbf{F}^{\mathrm{T}}\mathbf{F} - \mathbf{I}) = \frac{1}{2}(\mathbf{u}_{,\mathrm{x}}^{\mathrm{T}} + \mathbf{u}_{,\mathrm{x}} + \mathbf{u}_{,\mathrm{x}}^{\mathrm{T}}\mathbf{u}_{,\mathrm{x}}) \tag{3}$$

- rate form of constitutive equation:

$$\mathbf{S}' = C.\mathbf{E}' \tag{4}$$

S, **F** and **E** are the second Piola–Kirchhoff stress tensor, the material deformation gradient and the Green–Lagrange strain tensor, respectively; **x** and $\bar{\mathbf{x}}$ denote the position vectors of an arbitrary point of the shell body in the reference and deformed configuration (Figure 1); **u** is the displacement field. **r**, $\bar{\mathbf{r}}$ and **v** are the corresponding variables of the reference surface. In view of an incremental formulation the constitutive law is required only in rate form. Its integration leads to total stresses.

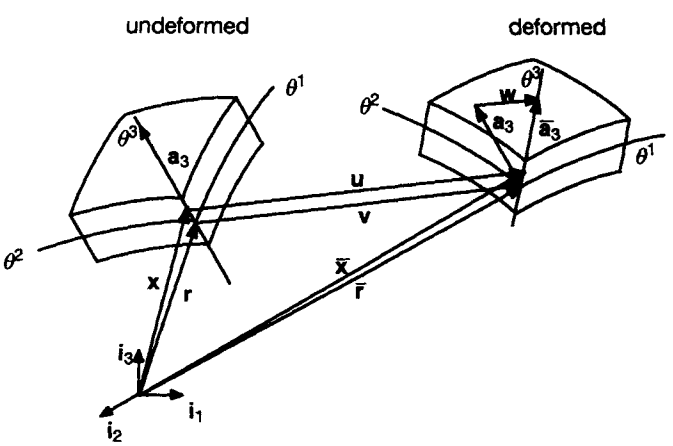

Figure 1. Deformation of the shell

An assumption for the displacement field across the thickness reduces the theory to its 2D-equivalent. Small transverse shear deformations justify a linear displacement field:

Assumption A1: $$\mathbf{u} = \bar{\mathbf{x}} - \mathbf{x} = \mathbf{v} + \theta^3 \mathbf{w} \tag{5}$$

The position vector of the deformed shell is

$$\bar{\mathbf{x}} = \mathbf{r} + \mathbf{v} + \theta^3(\mathbf{a}_3 + \mathbf{w}) = \bar{\mathbf{r}} + \theta^3 \bar{\mathbf{a}}_3, \quad -\frac{h}{2} \leqslant \theta^3 \leqslant \frac{h}{2} \tag{6}$$

h is the shell thickness. The shifter $\mathbf{Z}$ maps all variables to the metric of the reference surface:

$$\mathbf{Z} = \mathbf{x}_{,\mathrm{r}} = \mathbf{J}\mathbf{J}_0^{-1} \tag{7}$$

The Jacobians $\mathbf{J}$ of the shell space and $\mathbf{J}_0$ of the reference surface are derived from

$$\mathbf{J} = \frac{\partial \mathbf{x}}{\partial \boldsymbol{\theta}} = [\mathbf{g}_1, \mathbf{g}_2, \mathbf{g}_3] \qquad \mathbf{J}_0 = \mathbf{J}(\theta^3 = 0) = [\mathbf{a}_1, \mathbf{a}_2, \mathbf{a}_3]; \quad \boldsymbol{\theta} = [\theta^1, \theta^2, \theta^3] \tag{8}$$

where the column vectors are the covariant base vectors. The contravariant base vectors are obtained as columns of $\mathbf{J}^{-\mathrm{T}}$ and $\mathbf{J}_0^{-\mathrm{T}}$. $\mathbf{Z}$ and $\mathbf{J}$ are linear in θ^3:

$$\mathbf{Z} = \mathbf{x}_{,\mathrm{r}} = (\mathbf{r} + \theta^3 \mathbf{a}_3)_{,\mathrm{r}} = \mathbf{r}_{,\mathrm{r}} + \mathbf{a}_3 \theta^3_{,\mathrm{r}} + \theta^3 \mathbf{a}_{3,\mathrm{r}} = \mathbf{I} - \theta^3 \mathbf{B} \tag{9}$$

Here $\mathbf{I}$ defines the identity tensor; $\mathbf{B}$ is the symmetrical curvature tensor of the reference surface ($\mathbf{a}_3$ orthogonal to $\mathbf{a}_1$ and $\mathbf{a}_2$):

$$\mathbf{B} = -\mathbf{a}_{3,\mathrm{r}} = -\mathbf{a}_{3,\alpha} \otimes \mathbf{a}^{\alpha} = b_{\beta\alpha} \mathbf{a}^{\beta} \otimes \mathbf{a}^{\alpha} \quad \text{with:} \quad b_{\beta\alpha} = -\mathbf{a}_{3,\alpha} \mathbf{a}_{\beta} \tag{10}$$

Greek indices are either 1 or 2; Latin indices run from 1 to 3. The material deformation gradient can be decomposed by applying the chain rule:

$$\mathbf{F} = \bar{\mathbf{x}}_{,\mathrm{r}} \mathbf{r}_{,\mathrm{x}} = \hat{\mathbf{F}} \mathbf{Z}^{-1} \tag{11}$$

As a consequence of assumption A1 $\hat{\mathbf{F}}$ consists of a constant and a linear term:

$$\hat{\mathbf{F}} = \bar{\mathbf{x}}_{,\mathrm{r}} = \mathbf{x}_{,\mathrm{r}} + \mathbf{u}_{,\mathrm{r}} = \mathbf{F}_{\mathrm{C}} + \theta^3 \mathbf{F}_{\mathrm{L}} \tag{12}$$

with

$$\mathbf{F}_{\mathrm{C}} = \mathbf{I} + \mathbf{v}_{,\mathrm{r}} + \mathbf{w} \otimes \mathbf{a}_3 = \bar{\mathbf{a}}_i \otimes \mathbf{a}^i \tag{13}$$

$$\mathbf{F}_{\mathrm{L}} = \mathbf{w}_{,\mathrm{r}} - \mathbf{B} = \bar{\mathbf{a}}_{3,\mathrm{r}} = \bar{\mathbf{a}}_{3,\alpha} \otimes \mathbf{a}^{\alpha} \tag{14}$$

Introducing equations (9) and (11) into equation (3) leads to the Green–Lagrange strains

$$\begin{aligned} \mathbf{E} &= \mathbf{Z}^{-\mathrm{T}} \tfrac{1}{2} (\hat{\mathbf{F}}^{\mathrm{T}} \hat{\mathbf{F}} - \mathbf{Z}^{\mathrm{T}} \mathbf{Z}) \mathbf{Z}^{-1} = \mathbf{Z}^{-\mathrm{T}} \hat{\mathbf{E}} \mathbf{Z}^{-1} \\ &= \mathbf{Z}^{-\mathrm{T}} \tfrac{1}{2} (\mathbf{u}_{,\mathrm{r}}^{\mathrm{T}} \mathbf{Z} + \mathbf{Z}^{\mathrm{T}} \mathbf{u}_{,\mathrm{r}} + \mathbf{u}_{,\mathrm{r}}^{\mathrm{T}} \mathbf{u}_{,\mathrm{r}}) \mathbf{Z}^{-1} \\ &= \mathbf{Z}^{-\mathrm{T}} \tfrac{1}{2} (\mathbf{u}_{,\mathrm{r}}^{\mathrm{T}} + \mathbf{u}_{,\mathrm{r}} + \mathbf{u}_{,\mathrm{r}}^{\mathrm{T}} \mathbf{u}_{,\mathrm{r}} + \theta^3 (-\mathbf{u}_{,\mathrm{r}}^{\mathrm{T}} \mathbf{B} - \mathbf{B} \mathbf{u}_{,\mathrm{r}})) \mathbf{Z}^{-1} \end{aligned} \tag{15}$$

$\hat{\mathbf{E}}$ is quadratic in θ^3.

$$\hat{\mathbf{E}} = \hat{\mathbf{E}}_{\mathrm{C}} + \theta^3 \hat{\mathbf{E}}_{\mathrm{L}} + (\theta^3)^2 \hat{\mathbf{E}}_{\mathrm{Q}} \tag{16}$$

with

$$\hat{\mathbf{E}}_C = \tfrac{1}{2}(\mathbf{F}_C^T\mathbf{F}_C - \mathbf{I})$$
$$= \tfrac{1}{2}(\mathbf{v}_{,r}^T + \mathbf{v}_{,r} + \mathbf{w}\otimes\mathbf{a}_3 + \mathbf{a}_3\otimes\mathbf{w}$$
$$+ \mathbf{v}_{,r}^T\mathbf{v}_{,r} + \mathbf{v}_{,r}^T(\mathbf{w}\otimes\mathbf{a}_3) + (\mathbf{a}_3\otimes\mathbf{w})\mathbf{v}_{,r} + (\mathbf{a}_3\otimes\mathbf{w})(\mathbf{w}\otimes\mathbf{a}_3)) \tag{17}$$

$$\hat{\mathbf{E}}_L = \tfrac{1}{2}(\mathbf{F}_C^T\mathbf{F}_L + \mathbf{F}_L^T\mathbf{F}_C + \mathbf{B}^T + \mathbf{B})$$
$$= \tfrac{1}{2}(\mathbf{w}_{,r}^T + \mathbf{w}_{,r} - \mathbf{v}_{,r}^T\mathbf{B} - \mathbf{B}^T\mathbf{v}_{,r} - \mathbf{B}^T(\mathbf{w}\otimes\mathbf{a}_3) - (\mathbf{a}_3\otimes\mathbf{w})\mathbf{B}$$
$$+ \mathbf{w}_{,r}^T\mathbf{v}_{,r} + \mathbf{v}_{,r}^T\mathbf{w}_{,r} + \mathbf{w}_{,r}^T(\mathbf{w}\otimes\mathbf{a}_3) + (\mathbf{a}_3\otimes\mathbf{w})\mathbf{w}_{,r}) \tag{18}$$

$$\hat{\mathbf{E}}_Q = \tfrac{1}{2}(\mathbf{F}_L^T\mathbf{F}_L - \mathbf{B}^T\mathbf{B}) = \tfrac{1}{2}(-\mathbf{w}_{,r}^T\mathbf{B} - \mathbf{B}^T\mathbf{w}_{,r} + \mathbf{w}_{,r}^T\mathbf{w}_{,r}) \tag{19}$$

Dropping the underlined terms renders a geometrically linear theory.

The Piola–Kirchhoff stress tensor of the second kind is transformed to the reference surface as well: $\hat{\mathbf{S}} = \mathbf{Z}^{-1}\mathbf{S}\mathbf{Z}^{-T}$. Equations (15) and (16) are introduced into the virtual work expression, equation (1), denoting the determinant of the shifter by $\mu = \det\mathbf{Z} = \det\mathbf{J}/\det\mathbf{J}_0$:

$$\iiint_V \mathbf{S}\cdot\delta\mathbf{E}\,dV = \iiint_V \mathbf{S}\cdot\mathbf{Z}^{-T}\delta\hat{\mathbf{E}}\mathbf{Z}^{-1}\,dV$$
$$= \iint_A \left(\int_{-h/2}^{h/2}\mu\hat{\mathbf{S}}\,d\theta^3\right)\cdot\delta\hat{\mathbf{E}}_C + \left(\int_{-h/2}^{h/2}\mu\hat{\mathbf{S}}\theta^3\,d\theta^3\right)\cdot\delta\hat{\mathbf{E}}_L$$
$$+ \left(\int_{-h/2}^{h/2}\mu\hat{\mathbf{S}}(\theta^3)^2 d\theta^3\right)\cdot\delta\hat{\mathbf{E}}_Q\,dA$$
$$= \iint_A \tilde{\mathbf{N}}\cdot\delta\hat{\mathbf{E}}_C + \mathbf{M}\cdot\delta\hat{\mathbf{E}}_L + \mathbf{L}\cdot\delta\hat{\mathbf{E}}_Q\,dA \tag{20}$$

$\tilde{\mathbf{N}}$ denotes the pseudo-stress resultant tensor; the tilde is used to indicate that $\tilde{\mathbf{N}}$ is symmetric opposite to its physical counterpart $\mathbf{N}$. Although this holds also for $\mathbf{M}$, it is usually not distinguished. In view of a Newton-type iteration, equation (20) is usually linearized; since this process is a conventional process it will not be discussed here further. Now the constitutive equations for materials varying across the thickness can be defined in rate form for stress resultants.

$$\begin{bmatrix}\tilde{\mathbf{N}}'\\ \mathbf{M}'\\ \mathbf{L}'\end{bmatrix} = \begin{bmatrix} D_0\cdot[\ldots] & D_1\cdot[\ldots] & D_2\cdot[\ldots]\\ D_1\cdot[\ldots] & D_2\cdot[\ldots] & D_3\cdot[\ldots]\\ D_2\cdot[\ldots] & D_3\cdot[\ldots] & D_4\cdot[\ldots]\end{bmatrix}\begin{bmatrix}\hat{\mathbf{E}}_C'\\ \hat{\mathbf{E}}_L'\\ \hat{\mathbf{E}}_Q'\end{bmatrix} \tag{21}$$

Here:

$$D_i\cdot[\ldots] = \int_{-h/2}^{h/2}\mu\mathbf{Z}^{-1}\mathbf{C}\cdot[\mathbf{Z}^{-T}\ldots\mathbf{Z}^{-1}]\mathbf{Z}^{-T}(\theta^3)^i\,d\theta^3 \tag{22}$$

is introduced as an abbreviation.

It should be noted that, except assumption A1, no further hypotheses have been used. $\mathbf{Z}^{-1} = \mathbf{Z}^{-T}$ and $\mathbf{J}^{-1}$, respectively, can be determined analytically, applying the theorem of Caley–Hamilton. This operation is in general not necessary since the material matrices $D_i\cdot[\ldots]$ are integrated numerically.

If a relative error in the order of h/R (h = shell thickness, $1/R$ = maximal principal curvature = $O(\|\mathbf{B}\|)$; $\|(\ldots)\|$ = spectral norm) is tolerated, the above equations may be substantially simplified (see Reference 5, which refers to the work of Koiter and John).

Assumption A2: Provided that the gradients of the shear strains are small, the terms of equation (16) quadratic in θ^3 can be neglected, i.e. $\hat{\mathbf{E}}_Q = \mathbf{0}$. Because of this the third term in equation (20) vanishes.

Assumption A3: μ is taken as unity and $\mathbf{Z}^{-1}$ as the identity tensor in equation (22):

$$\mu = \det \mathbf{Z} = \det \mathbf{J}/\det \mathbf{J}_0 \approx 1; \quad \mathbf{Z}^{-1} = \mathbf{Z}^{-T} \approx \mathbf{I}$$

This is equivalent to $\hat{\mathbf{S}} \approx \mathbf{S}$; $\hat{\mathbf{E}} \approx \mathbf{E}$, in the energy expression.

Assumption A4: The normal stresses in the thickness direction are neglected, i.e. $\mathbf{a}_3^T \mathbf{S} \mathbf{a}_3 = S^{33} = 0$. For small strains this assumption allows one to introduce an inextensional shell director, that is $|\bar{\mathbf{a}}_3| = 1$. This constraint reduces the 6-parametric theory (components of $\mathbf{v}$ and $\mathbf{w}$) to its 5-parametric subset. The assumption is verified through a condensation of the material law: $C \to C^*$. The resulting error is of the order of vh/R for Hooke's material law, with v as Poisson's ratio.

All four assumptions together lead to a first approximation of a geometrically non-linear shell theory for small strains including transverse shear deformation.[3,14] Based on curvilinear convective co-ordinates θ^i the kinematic equations are in vectorial notation:

$$\hat{\mathbf{E}}_C = \tfrac{1}{2}(\mathbf{F}_C^T \mathbf{F}_C - \mathbf{I}) = \alpha_{ij} \mathbf{a}^i \otimes \mathbf{a}^j \quad \text{with} \quad \alpha_{ij} = \tfrac{1}{2}(\bar{\mathbf{a}}_i \bar{\mathbf{a}}_j - \mathbf{a}_i \mathbf{a}_j)$$
$$\text{from A4 follows} \quad \alpha_{33} = 0 \tag{23}$$

$$\hat{\mathbf{E}}_L = \tfrac{1}{2}(\mathbf{F}_C^T \mathbf{F}_L + \mathbf{F}_L^T \mathbf{F}_C + \mathbf{B}^T + \mathbf{B}) = \beta_{ij} \mathbf{a}^i \otimes \mathbf{a}^j$$
$$\text{with} \quad \beta_{ij} = \tfrac{1}{2}(\bar{\mathbf{a}}_i \bar{\mathbf{a}}_{3,j} + \bar{\mathbf{a}}_{3,i} \bar{\mathbf{a}}_j - \mathbf{a}_i \mathbf{a}_{3,j} - \mathbf{a}_{3,i} \mathbf{a}_j)$$
$$\text{from A4 follows} \quad \bar{\mathbf{a}}_3 \bar{\mathbf{a}}_{3,\alpha} = 0, \quad \bar{\mathbf{a}}_{3,3} = \mathbf{0} \quad \text{thus} \quad \beta_{i3} = \beta_{3i} = 0 \tag{24}$$

2.1.2. Concept of degeneration.

(a) Numerical integration across thickness

Elements with a numerical thickness integration, e.g. see References 1 and 17, start directly from the equations of a continuum and apply only assumption A1 and mostly A4. Insofar, they are from the theoretical point of view at least as rigorous as the above described shell theory.

(b) Explicit integration across thickness

- Integration due to Zienkiewicz–Taylor–Too (Z & T & T)

In order to improve the numerical efficiency, in particular for materials with varying properties across the thickness of a shell, the authors in Reference 28 proposed an explicit integration analogous to a shell theory, i.e. equation (21). They introduced the assumption

$$\mathbf{J} = \mathbf{J}_0 \tag{25}$$

which is equivalent to $\mathbf{Z} = \mathbf{I}$ and $\mathbf{B} = \mathbf{0}$ in the present notation.

$$\mathbf{E} = \tfrac{1}{2}(\mathbf{u}_{,x}^T + \mathbf{u}_{,x} + \mathbf{u}_{,x}^T \mathbf{u}_{,x}) = \tfrac{1}{2}(\mathbf{Z}^{-T} \mathbf{u}_{,r}^T + \mathbf{u}_{,r} \mathbf{Z}^{-1} + \mathbf{Z}^{-T} \mathbf{u}_{,r}^T \mathbf{u}_{,r} \mathbf{Z}^{-1})$$
$$\approx \tfrac{1}{2}(\mathbf{u}_{,r}^T + \mathbf{u}_{,r} + \mathbf{u}_{,r}^T \mathbf{u}_{,r}) = \mathbf{E}^{\approx} \tag{26}$$

This approximation is too restrictive, as can be concluded by a comparison with the shell formulation. It follows from assumption A3 and equation (15) that

$$\mathbf{E} \approx \hat{\mathbf{E}} = \mathbf{E}^{\approx} + \theta^3 \tfrac{1}{2}(-\mathbf{u}_{,r}^{\mathrm{T}}\mathbf{B} - \mathbf{B}\mathbf{u}_{,r}) \tag{27}$$

It should be pointed out that all missing terms ought to appear already in a geometrically linear theory. The dropped terms may cause unreasonably large errors for rigid body movements.

- Integration due to Milford–Schnobrich (M & S).

Milford and Schnobrich[12] have stressed the significance of the terms with **B**. Belytschko et al.[6] also emphasized the curvature terms; they demonstrated for the benchmark 'pre-twisted beam' that an error of up to 70 per cent may occur (see Example 2.3.1). The remedy in Reference 12 is a series expansion of $\mathbf{J}^{-1}$ cut off after the linear term. This is equivalent to the approximation

$$\mathbf{Z}^{-1} \approx \mathbf{I} + \theta^3\mathbf{B} \tag{28}$$

so that the strain tensor is

$$\begin{aligned}\mathbf{E} &\approx \tfrac{1}{2}((\mathbf{I} + \theta^3\mathbf{B})\mathbf{u}_{,r}^{\mathrm{T}} + \mathbf{u}_{,r}(\mathbf{I} + \theta^3\mathbf{B}) + (\mathbf{I} + \theta^3\mathbf{B})\mathbf{u}_{,r}^{\mathrm{T}}\mathbf{u}_{,r}(\mathbf{I} + \theta^3\mathbf{B}))\\ &= \tfrac{1}{2}(\mathbf{u}_{,r}^{\mathrm{T}} + \mathbf{u}_{,r} + \mathbf{u}_{,r}^{\mathrm{T}}\mathbf{u}_{,r} + \theta^3(\mathbf{B}\mathbf{u}_{,r}^{\mathrm{T}} + \mathbf{u}_{,r}\mathbf{B})\\ &\quad + \theta^3(\mathbf{B}\mathbf{u}_{,r}^{\mathrm{T}}\mathbf{u}_{,r} + \mathbf{u}_{,r}^{\mathrm{T}}\mathbf{u}_{,r}\mathbf{B}) + (\theta^3)^2\mathbf{B}\mathbf{u}_{,r}^{\mathrm{T}}\mathbf{u}_{,r}\mathbf{B})\end{aligned} \tag{29}$$

Using $\mathbf{u}_{,r} = \mathbf{v}_{,r} + \mathbf{w} \otimes \mathbf{a}_3 + \theta^3\mathbf{w}_{,r}$ and neglecting the terms quadratic and higher in θ^3 we get ($\mathbf{B}\mathbf{a}_3 = \mathbf{0}$):

$$\begin{aligned}\mathbf{E}^{\approx\approx} &= \tfrac{1}{2}(\mathbf{v}_{,r}^{\mathrm{T}} + \mathbf{v}_{,r} + \mathbf{w} \otimes \mathbf{a}_3 + \mathbf{a}_3 \otimes \mathbf{w}\\ &\quad + \mathbf{v}_{,r}^{\mathrm{T}}\mathbf{v}_{,r} + \mathbf{v}_{,r}^{\mathrm{T}}(\mathbf{w} \otimes \mathbf{a}_3) + (\mathbf{a}_3 \otimes \mathbf{w})\mathbf{v}_{,r} + (\mathbf{a}_3 \otimes \mathbf{w})(\mathbf{w} \otimes \mathbf{a}_3)\\ &\quad + \theta^3(\mathbf{w}_{,r}^{\mathrm{T}} + \mathbf{w}_{,r} + \mathbf{w}_{,r}^{\mathrm{T}}\mathbf{v}_{,r} + \mathbf{v}_{,r}^{\mathrm{T}}\mathbf{w}_{,r} + \mathbf{w}_{,r}^{\mathrm{T}}(\mathbf{w} \otimes \mathbf{a}_3) + (\mathbf{a}_3 \otimes \mathbf{w})\mathbf{w}_{,r})\\ &\quad + \theta^3(\mathbf{B}\mathbf{v}_{,r}^{\mathrm{T}} + \mathbf{v}_{,r}\mathbf{B} + \mathbf{B}\mathbf{v}_{,r}^{\mathrm{T}}\mathbf{v}_{,r} + \mathbf{B}\mathbf{v}_{,r}^{\mathrm{T}}(\mathbf{w} \otimes \mathbf{a}_3) + \mathbf{v}_{,r}^{\mathrm{T}}\mathbf{v}_{,r}\mathbf{B} + (\mathbf{a}_3 \otimes \mathbf{w})\mathbf{v}_{,r}\mathbf{B})\end{aligned} \tag{30}$$

Since $\mathbf{E}^{\approx}$, $\mathbf{E}^{\approx\approx}$ and $\hat{\mathbf{E}}$ do not differ in the constant terms, the part linear in θ^3 will be closer looked at:

$$\mathbf{E}_{\mathrm{L}}^{\approx} = \tfrac{1}{2}(\mathbf{w}_{,r}^{\mathrm{T}} + \mathbf{w}_{,r} + \mathbf{w}_{,r}^{\mathrm{T}}\mathbf{v}_{,r} + \mathbf{v}_{,r}^{\mathrm{T}}\mathbf{w}_{,r} + \mathbf{w}_{,r}^{\mathrm{T}}(\mathbf{w} \otimes \mathbf{a}_3) + (\mathbf{a}_3 \otimes \mathbf{w})\mathbf{w}_{,r}) \tag{31}$$

$$\hat{\mathbf{E}}_{\mathrm{L}} = \mathbf{E}_{\mathrm{L}}^{\approx} + \tfrac{1}{2}(-\mathbf{v}_{,r}^{\mathrm{T}}\mathbf{B} - \mathbf{B}\mathbf{v}_{,r} - \mathbf{B}(\mathbf{w} \otimes \mathbf{a}_3) - (\mathbf{a}_3 \otimes \mathbf{w})\mathbf{B}) \tag{32}$$

$$\mathbf{E}_{\mathrm{L}}^{\approx\approx} = \mathbf{E}_{\mathrm{L}}^{\approx} + \tfrac{1}{2}(\mathbf{B}\mathbf{v}_{,r}^{\mathrm{T}} + \mathbf{v}_{,r}\mathbf{B} + \mathbf{B}\mathbf{v}_{,r}^{\mathrm{T}}\mathbf{v}_{,r} + \mathbf{B}\mathbf{v}_{,r}^{\mathrm{T}}(\mathbf{w} \otimes \mathbf{a}_3) + \mathbf{v}_{,r}^{\mathrm{T}}\mathbf{v}_{,r}\mathbf{B} + (\mathbf{a}_3 \otimes \mathbf{w})\mathbf{v}_{,r}\mathbf{B}) \tag{33}$$

Equations (32) and (33) differ only slightly because:

$$\begin{aligned}\|\mathbf{E}_{\mathrm{L}}^{\approx\approx} - \hat{\mathbf{E}}_{\mathrm{L}}\| &= \|\mathbf{B}(\mathbf{v}_{,r}^{\mathrm{T}} + \mathbf{v}_{,r} + \mathbf{w} \otimes \mathbf{a}_3 + \mathbf{v}_{,r}^{\mathrm{T}}\mathbf{v}_{,r} + \mathbf{v}_{,r}^{\mathrm{T}}(\mathbf{w} \otimes \mathbf{a}_3))\\ &\quad + (\mathbf{v}_{,r}^{\mathrm{T}} + \mathbf{v}_{,r} + \mathbf{a}_3 \otimes \mathbf{w} + \mathbf{v}_{,r}^{\mathrm{T}}\mathbf{v}_{,r} + (\mathbf{a}_3 \otimes \mathbf{w})\mathbf{v}_{,r})\mathbf{B}\|\\ &= \|\mathbf{B}\hat{\mathbf{E}}_{\mathrm{C}} + \hat{\mathbf{E}}_{\mathrm{C}}\mathbf{B}\| \leqslant \frac{2}{R}\eta \quad \text{with} \quad O(\|\hat{\mathbf{E}}_{\mathrm{C}}\|) \leqslant O(\|\hat{\mathbf{E}}\|) = \eta\end{aligned} \tag{34}$$

Hence, the relative difference between $\mathbf{E}_{\mathrm{C}+\mathrm{L}}^{\approx\approx}$ and $\hat{\mathbf{E}}_{\mathrm{C}+\mathrm{L}}$ is of the order of $\theta^3 \dfrac{2}{R} \leqslant \dfrac{h}{R}$. For the special case of a geometrically linear theory we have:

$$\hat{\mathbf{E}}_{\mathrm{C}}^{\mathrm{lin}} = (\mathbf{v}_{,r} + \mathbf{w} \otimes \mathbf{a}_3)^{\mathrm{sym}} = \tfrac{1}{2}(\mathbf{v}_{,r}^{\mathrm{T}} + \mathbf{v}_{,r} + \mathbf{w} \otimes \mathbf{a}_3 + \mathbf{a}_3 \otimes \mathbf{w}) \tag{35}$$

$\hat{\mathbf{E}}_L$ can now be expressed as:

$$\hat{\mathbf{E}}_L = \mathbf{E}_L^{\approx} - \tfrac{1}{2}(\mathbf{B}\hat{\mathbf{E}}_C^{\text{lin}} + \hat{\mathbf{E}}_C^{\text{lin}}\mathbf{B}) - \tfrac{1}{2}(\mathbf{B}(\mathbf{v}_{,r} + \mathbf{w} \otimes \mathbf{a}_3)^{\text{skew}} - (\mathbf{v}_{,r} + \mathbf{w} \otimes \mathbf{a}_3)^{\text{skew}}\mathbf{B})$$
$$\approx \mathbf{E}_L^{\approx} - \tfrac{1}{2}(\mathbf{B}(\mathbf{v}_{,r} + \mathbf{w} \otimes \mathbf{a}_3)^{\text{skew}} - (\mathbf{v}_{,r} + \mathbf{w} \otimes \mathbf{a}_3)^{\text{skew}}\mathbf{B}) \tag{36}$$

The skew symmetric part $(\mathbf{v}_{,r} + \mathbf{w} \otimes \mathbf{a}_3)^{\text{skew}}$ represents the rigid modes in a linear theory and thus explains the noticeable error, e.g. for the 'pre-twisted beam'.

In order to judge the significance of the extra terms $-\mathbf{B}(\mathbf{w} \otimes \mathbf{a}_3) - (\mathbf{a}_3 \otimes \mathbf{w})\mathbf{B}$ in $\hat{\mathbf{E}}_L$ the components of $\mathbf{E}_L^{\approx}$ in a local basis are investigated:

$$\beta_{\alpha\beta}^{\approx} = \mathbf{a}_\alpha \mathbf{E}_L^{\approx} \mathbf{a}_\beta = \tfrac{1}{2}(\mathbf{w}_{,\alpha}\mathbf{a}_\beta + \mathbf{w}_{,\beta}\mathbf{a}_\alpha + \mathbf{w}_{,\alpha}\mathbf{v}_{,\beta} + \mathbf{w}_{,\beta}\mathbf{v}_{,\beta}) \tag{37}$$

$$\beta_{\alpha 3}^{\approx} = \mathbf{a}_\alpha \mathbf{E}_L^{\approx} \mathbf{a}_3 = \mathbf{a}_\alpha \tfrac{1}{2}(\mathbf{w}_{,r}^{\mathrm{T}}\mathbf{a}_3 + \mathbf{w}_{,r}^{\mathrm{T}}\mathbf{w}) \overset{\text{with A4}}{=} \tfrac{1}{2}(\mathbf{a}_\alpha \mathbf{B}\mathbf{w}) \neq 0; \quad \beta_{33} = 0 \tag{38}$$

Although necessarily the curvatures $\beta_{\alpha 3}^{\approx}$ do not vanish despite assumption A4. In a local formulation $\beta_{\alpha 3}^{\approx}$ is a priori not considered. This automatically avoids the above indicated error. Contrary to $\mathbf{E}_L^{\approx}$ $\hat{\beta}_{\alpha 3}$ does vanish in $\hat{\mathbf{E}}_L$ (see also equation (24)).

$$\hat{\beta}_{\alpha 3} = \beta_{\alpha 3}^{\approx} + \mathbf{a}_\alpha \tfrac{1}{2}(-\mathbf{B}\mathbf{w}) = 0 \tag{39}$$

If global Cartesian coordinates are used $\beta_{\alpha 3}^{\approx}$ cannot be isolated and individually neglected; therefore the extra terms $-\mathbf{B}(\mathbf{w} \otimes \mathbf{a}_3) - (\mathbf{a}_3 \otimes \mathbf{w})\mathbf{B}$ in $\hat{\mathbf{E}}_L$ need to be taken into account (see example 2.3.2).

For the sake of completeness also $\mathbf{E}_L^{\approx\,\approx}$ will be looked at:

$$\beta_{\alpha 3}^{\approx\,\approx} = \beta_{\alpha 3}^{\approx} + \mathbf{a}_\alpha \tfrac{1}{2}(\mathbf{B}\mathbf{v}_{,r}^{\mathrm{T}}\mathbf{a}_3) = \mathbf{a}_\alpha \tfrac{1}{2}\mathbf{B}(\mathbf{w} + \mathbf{v}_{,r}^{\mathrm{T}}\mathbf{a}_3) = \tfrac{1}{2}\mathbf{a}_\alpha \mathbf{B}\gamma^{\text{lin}} \approx 0 \tag{40}$$

γ^{lin} denotes the transverse shear deformation in a geometrically linear theory.

- Integration due to Irons

Irons derived in 1973[11] the bending strains of his 'Semi-Loof' shell element—based on local Cartesian co-ordinates—from the strains at the upper and lower shell surfaces. If the discretization already introduced by Irons at this stage is filtered out, the resulting terms coincide exactly with the bending strains $\hat{\mathbf{E}}_L$ of the shell theory. At that time he obviously was not aware of the relevance of this part because he says: 'In the solution to a real problem it is probably an order of magnitude smaller than the orthodox bending terms. It is questionable therefore whether it should be included, . . . '. And with respect to the derivation he mentions: 'There is more engineering intuition than mathematics in this step.'

Crisfield[9] follows a similar idea to obtain the curvature terms for a 2-dimensional beam element. As a consequence the rigid body movements can be described without defect.

- Integration due to Stanley

Finally, we wish to refer to a paper of Stanley[26] in which $\mathbf{Z}^{-1}$ is completely taken into consideration and $\hat{\mathbf{E}}_Q$ is not neglected. The results are identical to those obtained by a numerically integrated version. But it should be noted that not all terms need to be included if a relative error of the order of h/R is tolerated and the analysis is restricted to small strains as well as slightly varying thickness.

2.1.3. Conclusion for explicit integration. It has been shown how the explicit integration across the thickness can be classified under the aspect of a shell theory. The strain tensor $\hat{\mathbf{E}}$ ought to be preferred since consistent shell theory and explicit integration coincide. Then a series expansion of $\mathbf{J}^{-1}$ and $\mathbf{Z}^{-1}$, resp., is unnecessary; the derivation is mathematically consistent, unnecessary terms are not carried along.

The only difference between the concept of degeneration and shell theory based finite elements remains in the kind of discretization. The way described by Simo and co-workers[20-23] is also preferred here: it is started from the strain definitions of shell theory, equations (23) and (24), but a discretization typical for the degeneration concept is introduced (see also Reference 13). At this point we would like to stress that a 6-parameter theory may be useful in the case of rather thick structures and for large strain problems.[23] An explicit integration in the thickness direction referring also to higher order stress resultants may be computationally advantageous even in those cases, especially for layered structures.

2.2. *Comparison of discretization*

2.2.1. Shell theory. It is common in shell theory that the initial geometry is analytically defined by applying the classical means of differential geometry. However, any other geometrical parameterization is possible, for example isoparametric interpolation. The often heard argument that the extreme sensitivity with respect to initial geometrical imperfections in shell stability is very much influenced by this parameterization is not shared herein. The errors introduced by an approximation of initial and deformed geometry will be of the same order of magnitude. The deformed geometry is indirectly interpolated through the displacement field.

$$\mathbf{u} = \bar{\mathbf{x}} - \tilde{\mathbf{x}} = \mathbf{v} + \theta^3 \mathbf{w} = \mathbf{v} + \theta^3(\mathbf{R}(\mathbf{s}) - \mathbf{I})\mathbf{a}_3 \tag{41}$$

Usually the components of $\mathbf{v}$ and $\mathbf{s}$ with respect to the local basis $\mathbf{a}_i$ are discretized:

$$\mathbf{v} \approx \mathbf{v}_h = \left(\sum_{k=1}^{n} N^k (v^i)^k \right) \mathbf{a}_i; \quad \mathbf{s} \approx \mathbf{s}_h = \left(\sum_{k=1}^{n} N^k (s^\alpha)^k \right) \mathbf{a}_\alpha \tag{42}$$

This kind of interpolation automatically causes difficulties with the rigid body modes of curved structures which, in turn, diminish with a finer discretization. Alternative kinds of interpolation are possible, e.g. with respect to other base vectors.

2.2.2. Concept of degeneration. Usually in the degeneration approach initial and deformed geometry are equally interpolated, allowing one to describe rigid body movements exactly:

$$\mathbf{x} \approx \mathbf{x}_h = \sum_{k=1}^{n} N^k (\mathbf{r} + \theta^3 \mathbf{a}_3)^k; \quad \tilde{\mathbf{x}} \approx \tilde{\mathbf{x}}_h = \sum_{k=1}^{n} N^k (\bar{\mathbf{r}} + \theta^3 \bar{\mathbf{a}}_3)^k \tag{43}$$

The displacement field follows:

$$\mathbf{u} \approx \mathbf{u}_h = \sum_{k=1}^{n} N^k (\mathbf{v} + \theta^3 \mathbf{w})^k \tag{44}$$

Assuming constant shell thickness leads to

$$\mathbf{v} \approx \mathbf{v}_h = \left(\sum_{k=1}^{n} N^k (v^i)^k \right) \mathbf{i}_i; \quad \mathbf{w} \approx \mathbf{w}_h = \left(\sum_{k=1}^{n} N^k (\mathbf{w}^i)^k \right) \mathbf{i}_i \tag{45}$$

and

$$\bar{\mathbf{r}} \approx \bar{\mathbf{r}}_h = \sum_{k=1}^{n} N^k \bar{\mathbf{r}}^k; \qquad \bar{\mathbf{a}}_3 \approx \bar{\mathbf{a}}_{3_h} = \sum_{k=1}^{n} N^k \bar{\mathbf{a}}_3^k \tag{46}$$

respectively.

This kind of interpolation causes the defect that the assumption $|\bar{\mathbf{a}}_3| = 1$ is violated at each Gauss point. The element turns out to be too flexible, in particular for a coarse mesh and low order elements. Better results are obtianed if $\mathbf{s}$ instead of $\mathbf{w} = (\mathbf{R}(\mathbf{s}) - \mathbf{I})\mathbf{a}_3$ is interpolated[7,22] (see Example 2.3.3).

$$\mathbf{s} \approx \mathbf{s}_h = \left(\sum_{k=1}^{n} N^k (s^i)^k \right) \mathbf{i}_i \tag{47}$$

However, the computation of the tangent stiffness matrix will be more expensive. Applying equation (46) also leads to the fact that $\mathbf{s}$ is not orthogonal to $\mathbf{a}_3$ at the Gauss points.

Again this defect diminishes when the mesh is refined or higher order elements are chosen.

An alternative scheme is used in Reference 21: $\bar{\mathbf{a}}_{3h}$ is normalized enforcing the condition $|\bar{\mathbf{a}}_3| = 1$.

2.3. *Numerical examples*

2.3.1. Twisted beam[6]*—Geometrically linear analysis.* This often described benchmark was chosen in Reference 6 and is repeated here. It demonstrates the significant error arising if the two terms $-\mathbf{v}_{,r}^{\mathrm{T}}\mathbf{B} - \mathbf{B}\mathbf{v}_{,r}$ are neglected in $\hat{\mathbf{E}}_{\mathrm{L}}$. (See Figure 2.)

2.3.2. Arch—Geometrically linear analysis. This example shows the error if the terms $-\mathbf{B}(\mathbf{w} \otimes \mathbf{a}_3) - (\mathbf{a}_3 \otimes \mathbf{w})\mathbf{B}$ are missing in equation (32). As mentioned above, this defect is automatically corrected in most local formulations, but does not vanish in formulations referring stresses and strains to global Cartesian co-ordinates. (See Figure 3.)

2.3.3. Cantilever beam—Geometrically non-linear analysis. This simple example demonstrates too weak behaviour if the director or respectively $\mathbf{w}$ is interpolated, so that the inextensibility requirement of the director is violated. An interpolation of $\mathbf{s}$ gives much better results,[7,22] but leads to a more elaborate formulation. One-point reduced integrated elements are used. The nodes in the width direction are coupled.

Young's modulus $E = 29*10^6$
Poisson's ratio $\nu = 0.22$
Length = 12 Thickness h
Width = 1.1 Load P
Twist = 90°

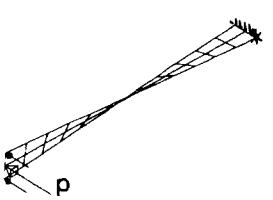

Mesh: 2x12 four-node elements, reduced integrated (1x1)

	h = 0.32, P = 1	h = 0.032, P = 10^{-6}
explicit integration due to Z&T&T (local):	0.2419×10^{-2}	0.2208×10^{-2}
explicit integration with $\hat{\mathbf{E}}$:	0.1887×10^{-2}	0.1281×10^{-2}
exact:	0.1754×10^{-2}	0.1294×10^{-2}

Figure 2. Twisted beam

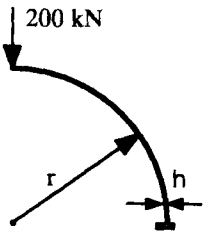

Mesh: 4 nine-node elements, reduced integrated (2x2)
(nodes in width direction are coupled)

Young's modulus E = 2.1 10^5 N/mm^2
Poisson's ratio ν = 0
Width b = 1000 mm ; Radius r = 5000 mm
Thickness h = 50 mm

displacement in load direction	
explicit integration due to Z&T&T (global):	3.834 mm
explicit integration with $\hat{\mathbf{E}}$:	5.714 mm
exact:	5.714 mm

Figure 3. Arch

Young's modulus E = 21000
Poisson's ratio ν=0.0
Length l = 100
Width b = 1.0
Thickness h = 2.0
Moment M = 879.6456

tip rotation:	**s** interpolated	**w** interpolated
10 four-node elements	361.94°	392.07°
20 four-node elements	361.94°	368.30°
exact:	361.94°	

Figure 4. Cantilever beam

Using Hooke's material law between the Biot stresses and engineering strains, the applied moment leads to a tip rotation of 360·00°.[7] However, if the material law uses Green–Lagrange strains and 2nd Piola–Kirchhoff stresses the exact result is 361·94° for these properties. (See Figure 4.)

3. LARGE ROTATIONS

3.1. Different options

3.1.1. Preliminary remarks. Large rotations can be completely described by one orthogonal tensor which in general depends on three independent variables. For shells the rotation around the normal is usually not considered so that only two independent variables exist. Several options exist for the kind of formulation; most of them are based either on elementary rotations or on a rotational vector.

3.1.2. Formulations based on elementary rotations. Elementary rotations are rotations around one axis.

$$\mathbf{R}_x(\alpha) = \begin{pmatrix} 1 & 0 & 0 \\ 0 & \cos\alpha & -\sin\alpha \\ 0 & \sin\alpha & \cos\alpha \end{pmatrix} \qquad \mathbf{R}_y(\beta) = \begin{pmatrix} \cos\beta & 0 & \sin\beta \\ 0 & 1 & 0 \\ -\sin\beta & 0 & \cos\beta \end{pmatrix}$$

$$\mathbf{R}_z(\gamma) = \begin{pmatrix} \cos\gamma & -\sin\gamma & 0 \\ \sin\gamma & \cos\gamma & 0 \\ 0 & 0 & 1 \end{pmatrix} \tag{48}$$

Among these are the versions based on

Euler angles: $$\mathbf{R} = \mathbf{R}_z(\phi)\mathbf{R}_x(\alpha)\mathbf{R}_z(\gamma) \tag{49}$$

and

Cardan angles: $$\mathbf{R} = \mathbf{R}_x(\alpha)\mathbf{R}_y(\beta)\mathbf{R}_z(\gamma) \tag{50}$$

but also the angles used by the second author in 1976 in large rotation shell analysis.[16,17] (See Figure 5.)

$$\mathbf{a}_3 = \mathbf{R}\mathbf{i}_y = \mathbf{R}_x(\alpha)\mathbf{R}_z\left(\beta - \frac{\pi}{2}\right)\mathbf{i}_y \tag{51}$$

Unfortunately all these formulations are not free of singularities. The uniqueness is lost for Eulerian angles at $\alpha = (k-1)\pi$, for Cardanian angles at $\beta = (2k-1)\pi/2$ and for the angles chosen in References 16 and 17 for $\beta = (k-1)\pi$, $k \in Z$.

3.1.3. Formulations based on rotational vector. Rotational vectors are strongly related to Euler parameters and quaternions. Both formulations start with four parameters to describe finite rotations but then, of course, an extra constraint comes in.

Euler parameters are based on the idea that each rotation can be described by a rotational axis and its related angle. (See Figure 6.) A vector parallel to the rotational axis is not changed during the rotation; thus it is an eigenvector of $\mathbf{R}$ with the eigenvalue $\lambda = 1$:

$$\mathbf{R}\mathbf{e} = \mathbf{e} \tag{52}$$

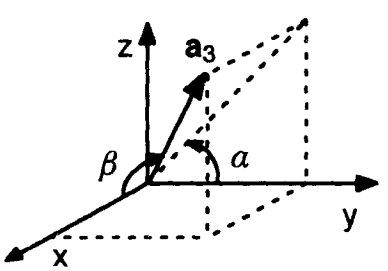

Figure 5. Rotations chosen in References 16 and 17

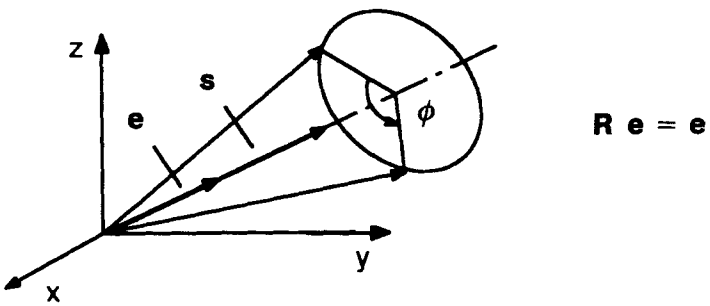

Figure 6. Euler parameters, rotational vector

The three components of vector **e** and angle ϕ define the Euler parameters. The extra constraint equation is

$$\mathbf{e}^T\mathbf{e} = 1 \tag{53}$$

The rotational tensor **R** can be uniquely determined from these parameters without any singularities.

$$\mathbf{R} = \mathbf{I} + \sin\phi\hat{\mathbf{e}} + (1 - \cos\phi)\hat{\mathbf{e}}\hat{\mathbf{e}} \tag{54}$$

Matrix $\hat{\mathbf{e}}$ in equation (54) operates on a vector like a cross product. For orthogonal Cartesian co-ordinates it follows that

$$\begin{gathered}\mathbf{e} = e_i\mathbf{i}^i \qquad \hat{\mathbf{e}} = \hat{e}_{ij}\mathbf{i}^i \otimes \mathbf{i}^j = (\mathbf{e}\times) \\ [e_i] = \begin{bmatrix} e_1 \\ e_2 \\ e_3 \end{bmatrix} \qquad [\hat{e}_{ij}] = \begin{bmatrix} 0 & -e_3 & e_2 \\ e_3 & 0 & -e_1 \\ -e_2 & e_1 & 0 \end{bmatrix}\end{gathered} \tag{55}$$

If the constraint equation (53) is directly applied in a numerical analysis, for example to eliminate $e_3 = \sqrt{1 - e_1^2 - e_2^2}$ leaving ϕ, e_1, e_2 as primary variables, e_3 may become numerically unstable.

The four quaternion parameters q_0, **q** are closely related to the Euler parameters.

$$q_0 = \cos\frac{\phi}{2} \qquad \mathbf{q} = \sin\frac{\phi}{2}\mathbf{e} \tag{56}$$

They lead straightforwardly to the rotational tensor **R**.

$$\mathbf{R} = \mathbf{I} + 2q_0\hat{\mathbf{q}} + 2\hat{\mathbf{q}}\hat{\mathbf{q}} \tag{57}$$

In finite element analyses the components of **q** can be used as primary variables; then $\mathbf{q}_0$ is determined by the constraint equation

$$q_0 = \sqrt{1 - \mathbf{q}^T\mathbf{q}} \tag{58}$$

Again, numerical sensitivities may occur here also.

As appeared to Euler or quaternion parameters, formulations with rotational vectors use only three parameters, i.e. the components of vector **s**. All alternatives differ only in the length of **s**.[15]

$$1.\ \mathbf{s}_1 = 2\tan\frac{\phi}{2}\mathbf{e} \qquad \rightarrow \mathbf{R} = \mathbf{I} + \frac{1}{1 + \dfrac{\mathbf{s}_1^{\mathrm{T}}\mathbf{s}_1}{4}}(\hat{\mathbf{s}}_1 + \hat{\mathbf{s}}_1\hat{\mathbf{s}}_1) \tag{59}$$

$$2.\ \mathbf{s}_2 = \tan\frac{\phi}{2}\mathbf{e} = \frac{\mathbf{q}}{q_0} \rightarrow \mathbf{R} = \mathbf{I} + \frac{2}{1 + \mathbf{s}_2^{\mathrm{T}}\mathbf{s}}(\hat{\mathbf{s}}_2 + \hat{\mathbf{s}}_2\hat{\mathbf{s}}_2) \tag{60}$$

$$3.\ \mathbf{s}_3 = \sin\phi\,\mathbf{e} \qquad \rightarrow \mathbf{R} = \mathbf{I} + \hat{\mathbf{s}}_3 + \frac{1}{2\cos^2\dfrac{\phi}{2}}\hat{\mathbf{s}}_3\hat{\mathbf{s}}_3 \tag{61}$$

$$4.\ \mathbf{s} = \phi\,\mathbf{e} \qquad \rightarrow \mathbf{R} = \mathbf{I} + \frac{\sin\phi}{\phi}\hat{\mathbf{s}} + \frac{1 - \cos\phi}{\phi^2}\hat{\mathbf{s}}\hat{\mathbf{s}} = \exp(\hat{\mathbf{s}}) \tag{62}$$

Each case has certain pros and cons, which are more or less relevant. For example, cases 1 and 2 lead to simple formulae for the total rotational vector emerging from two subsequent rotations but render an infinite length of the rotational vector at $\phi = (2k - 1)\pi$. Here also the third term of equation (61) of case 3 becomes unstable. Formulation 4, often attributed to Rodrigues, is the only one without singularities in the range of $0 \leqslant \phi < 2\pi$ because

$$\lim_{\phi\to 0}\frac{\sin\phi}{\phi} = 1 \qquad \lim_{\phi\to 0}\frac{1 - \cos\phi}{\phi^2} = \frac{1}{2} \tag{63}$$

3.2. Symmetry and asymmetry of the stiffness matrix for large rotations

If a Newton iteration is performed to solve the set of non-linear equations the tangent stiffness matrix has to be determined. In non-flat spaces the second Gateaux derivative of a potential is in general non-symmetric.[19,24] In Reference 19 Simo shows, after introducing a bi-invariant Riemannian metric, that the symmetric Hessian of the potential can be calculated by symmetrizing the second Gateaux derivative. Here we follow a different derivation leading directly to the same symmetric and non-symmetric matrices.

For simplicity it is assumed that the potential Π depends only on the rotations, i.e. $\Pi[\mathbf{R}(\mathbf{s})]$, with **s** as member of the flat Euclidian space $\mathbb{R}^3$.

In the following we use the abbreviations:

$$\delta\mathbf{f} = \frac{\mathrm{d}}{\mathrm{d}\varepsilon}\mathbf{f}(\mathbf{s} + \varepsilon\mathbf{s}^*)\bigg|_{\varepsilon=0}; \quad \mathrm{D}\mathbf{f} = \frac{\mathrm{d}}{\mathrm{d}\varepsilon}\mathbf{f}(\mathbf{s} + \varepsilon\mathbf{s}^+)\bigg|_{\varepsilon=0} \tag{64}$$

The potential becomes stationary if

$$\delta\Pi = \int_B \delta\pi\,\mathrm{d}B = \int_B \frac{\partial\pi}{\partial\mathbf{R}}\cdot\delta\mathbf{R}\,\mathrm{d}B = \int_B \frac{\partial\pi}{\partial\mathbf{R}}\cdot\mathbf{K}(\mathbf{s}, \mathbf{s}^*)\mathbf{R}\,\mathrm{d}B = 0 \tag{65}$$

Here **K** is a skew-symmetric matrix:

$$\mathbf{R}\mathbf{R}^{\mathrm{T}} = \mathbf{I} \rightarrow \delta\mathbf{R}\mathbf{R}^{\mathrm{T}} + \mathbf{R}\delta\mathbf{R}^{\mathrm{T}} = \mathbf{K} + \mathbf{K}^{\mathrm{T}} = \mathbf{O} \rightarrow \delta\mathbf{R} = \mathbf{K}(\mathbf{s}, \mathbf{s}^*)\mathbf{R} \tag{66}$$

The axial vector **k** related to **K** is given by

$$\mathbf{K}(\mathbf{s}, \mathbf{s}^*) = \hat{\mathbf{k}} = (\mathbf{k}\times) \qquad \mathbf{k} = \mathbf{T}(\mathbf{s})\mathbf{s}^* \tag{67}$$

Based on Rodrigues' formula, equation (62), $\mathbf{T}$ follows as

$$\mathbf{T}(\mathbf{s}) = \frac{\sin\phi}{\phi}\mathbf{I} + \frac{1-\cos\phi}{\phi^2}\hat{\mathbf{s}} + \left(\frac{1}{\phi^2} - \frac{\sin\phi}{\phi^3}\right)\mathbf{s}\otimes\mathbf{s} \tag{68}$$

For the tangent stiffness operator equation (65) has to be linearized with respect to $\mathbf{s}$:

$$\mathrm{D}\delta\Pi = \int_B \mathrm{D}\delta\pi\,\mathrm{d}B = \int_B \left[\delta\mathbf{R}\cdot\frac{\partial^2\pi}{\partial\mathbf{R}\,\partial\mathbf{R}}\cdot\mathrm{D}\mathbf{R} + \frac{\partial\pi}{\partial\mathbf{R}}\cdot\mathrm{D}\delta\mathbf{R}\right]\mathrm{d}B \tag{69}$$

The expression $\mathrm{D}\delta\mathbf{R}$ is determined by

$$\mathrm{D}\delta\mathbf{R} = (\mathrm{D}\mathbf{K}(\mathbf{s},\mathbf{s}^*) + \mathbf{K}(\mathbf{s},\mathbf{s}^*)\mathbf{K}(\mathbf{s},\mathbf{s}^+))\mathbf{R}(\mathbf{s}) \tag{70}$$

Because of $\mathrm{D}\mathbf{k} = \mathrm{D}\mathbf{T}(\mathbf{s})\mathbf{s}^*$ the directional derivative $\mathrm{D}\mathbf{K} = \mathrm{D}\hat{\mathbf{k}}$ requires the derivative $\mathrm{D}\mathbf{T}$, a very elaborate calculation.

$$\begin{aligned}\mathrm{D}\mathbf{T} = &\left(\frac{\phi\cos\phi - \sin\phi}{\phi^3}\mathbf{I} + \frac{-2+\phi\sin\phi+2\cos\phi}{\phi^4}\hat{\mathbf{s}}\right.\\ &\left.+\frac{(-2-\cos\phi)\phi + 3\sin\phi}{\phi^5}\mathbf{s}\otimes\mathbf{s}\right)\mathbf{s}^{\mathrm{T}}\mathbf{s}^+\\ &+\frac{1-\cos\phi}{\phi^2}\hat{\mathbf{s}}^+ + \left(\frac{1}{\phi^2} - \frac{\sin\phi}{\phi^3}\right)(\mathbf{s}^+\otimes\mathbf{s} + \mathbf{s}\otimes\mathbf{s}^+)\end{aligned} \tag{71}$$

After some reordering and using equations (65) and (71) the Hessian of Π results in

$$\mathrm{D}\delta\Pi = \int_B \left[\mathbf{K}^{*\mathrm{T}}\cdot\mathbf{R}\frac{\partial^2\tilde{\pi}}{\partial\mathbf{R}^{\mathrm{T}}\partial\mathbf{R}}\mathbf{R}^{\mathrm{T}}\cdot\mathbf{K}^+ + \frac{\partial\tilde{\pi}}{\partial\mathbf{R}}\mathbf{R}^{\mathrm{T}}\cdot(\mathrm{D}\mathbf{K}^* + \mathbf{K}^*\mathbf{K}^+)\right]\mathrm{d}B \tag{72}$$

with $\qquad \mathbf{K}^* = \mathbf{K}(\mathbf{s},\mathbf{s}^*) \qquad \mathbf{K}^+ = \mathbf{K}(\mathbf{s},\mathbf{s}^+)$

Although it is not obvious by simple inspection, equation (72) is after all symmetric with respect to $\mathbf{s}^*$ and $\mathbf{s}^+$. The expressions for $\mathbf{K}$ and $\mathrm{D}\mathbf{K}$ turn out to be extremely simple at $\mathbf{s} = \mathbf{0}$:

$$\mathbf{k}(\mathbf{0},\mathbf{s}^*) = \mathbf{s}^* \qquad \mathrm{D}\mathbf{k}(\mathbf{0},\mathbf{s}^*) = \tfrac{1}{2}\hat{\mathbf{s}}^+\mathbf{s}^* \tag{73}$$

Then $\mathrm{D}\delta\mathbf{R}$ is

$$\mathrm{D}\delta\mathbf{R}|_{\mathbf{s}=\mathbf{0}} = \tfrac{1}{2}(\hat{\mathbf{s}}^+\hat{\mathbf{s}}^*) + \hat{\mathbf{s}}^*\hat{\mathbf{s}}^+ = \tfrac{1}{2}(\hat{\mathbf{s}}^+\hat{\mathbf{s}}^* + \hat{\mathbf{s}}^*\hat{\mathbf{s}}^+) \tag{74}$$

In order to benefit from this simplification the Newton scheme is slightly modified as follows (see Figure 7 and References 24 and 26, 27):

$\delta\Pi(\mathbf{R}) = \delta\tilde{\Pi}(\mathbf{R}(\bar{\mathbf{s}})\mathbf{R}^i) = \mathbf{0}$

—linearization at position: $\bar{\mathbf{s}} = \mathbf{o}$

$$\mathrm{D}\delta\tilde{\Pi}|_{\bar{\mathbf{s}}=\mathbf{0}} = \int_B \underbrace{\left[\hat{\mathbf{s}}^{*\mathrm{T}}\cdot\mathbf{R}^i\frac{\partial^2\tilde{\pi}}{\partial\mathbf{R}^{\mathrm{T}}\partial\mathbf{R}}\mathbf{R}^{i\mathrm{T}}\cdot\hat{\mathbf{s}}^+ + \frac{\partial\tilde{\pi}}{\partial\mathbf{R}}\mathbf{R}^{i\mathrm{T}}\cdot\frac{1}{2}(\hat{\mathbf{s}}^*\hat{\mathbf{s}}^+ + \hat{\mathbf{s}}^+\hat{\mathbf{s}}^*)\right]}_{\text{symmetric}}\mathrm{d}B$$

—update

$\mathbf{R}^{i+1} = \mathbf{R}(\mathbf{s}^+)\mathbf{R}^i$

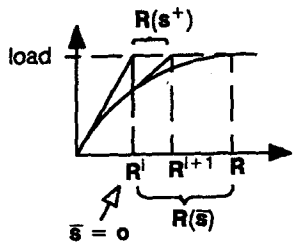

Figure 7

This procedure results in an algorithm which coincides with the symmetrized one of Simo and Vu-Quoc.[24] A similar approach is described by Cardona and Geradin,[8] although the multiplicative update is carried out only after every converged step.

The asymmetric tangent matrix presented in Reference 24 may be obtained through the following consideration:

$$\delta\Pi = \int_B \frac{\partial \pi}{\partial \mathbf{R}} \mathbf{R}^{\mathrm{T}} \cdot \mathbf{K}\, \mathrm{d}B = \int_B \hat{\mathbf{m}} \cdot \mathbf{K}\, \mathrm{d}B = \int_B 2\mathbf{m}^{\mathrm{T}}\mathbf{k}\, \mathrm{d}B = 0 \tag{75}$$

$$\text{with} \quad \hat{\mathbf{m}} = \operatorname{skew}\left(\frac{\partial \pi}{\partial \mathbf{R}} \mathbf{R}^{\mathrm{T}}\right)$$

Applying equation (67) and assuming that $\mathbf{T}^{-1}$ exists, it follows that

$$\int_B \mathbf{m}^{\mathrm{T}}\mathbf{k}\, \mathrm{d}B = \int_B \mathbf{m}^{\mathrm{T}}\mathbf{T}\mathbf{s}^*\, \mathrm{d}B = 0 \rightarrow \mathbf{m}^{\mathrm{T}}\mathbf{T} = \mathbf{0} \rightarrow \mathbf{m} = \mathbf{0} \tag{76}$$

For $\mathbf{m} = \mathbf{0}$ the potential Π is going to be stationary. Therefore, this condition may also read

$$\int_B 2\mathbf{m}^{\mathrm{T}}\mathbf{s}^*\, \mathrm{d}B = \int_B \frac{\partial \pi}{\partial \mathbf{R}} \mathbf{R}^{\mathrm{T}} \cdot \hat{\mathbf{s}}^*\, \mathrm{d}B = 0 \tag{77}$$

$\mathbf{s}^*$ can be considered as a test function. The linearization of this equation yields

$$\int_B \mathrm{D}\left(\frac{\partial \pi}{\partial \mathbf{R}} \mathbf{R}^{\mathrm{T}} \cdot \hat{\mathbf{s}}^*\right) \mathrm{d}B = \int_B \left[\hat{\mathbf{s}}^{*\mathrm{T}} \cdot \mathbf{R} \frac{\partial^2 \pi}{\partial \mathbf{R}^{\mathrm{T}} \partial \mathbf{R}} \mathbf{R}^{\mathrm{T}} \cdot \mathbf{K}^+ + \frac{\partial \pi}{\partial \mathbf{R}} \mathbf{R}^{\mathrm{T}} \cdot (\hat{\mathbf{s}}^* \mathbf{K}^+)\right] \mathrm{d}B \tag{78}$$

Again, the above described update of the rotation is applied:

$$\int_B \mathrm{D}\left(\frac{\partial \tilde{\pi}}{\partial \mathbf{R}} \mathbf{R}^{i\mathrm{T}} \cdot \hat{\mathbf{s}}^*\right) \mathrm{d}B = \int_B \left[\hat{\mathbf{s}}^{*\mathrm{T}} \cdot \mathbf{R}^i \frac{\partial^2 \tilde{\pi}}{\partial \mathbf{R}^{\mathrm{T}} \partial \mathbf{R}} \mathbf{R}^{i\mathrm{T}} \cdot \hat{\mathbf{s}}^+ + \frac{\partial \tilde{\pi}}{\partial \mathbf{R}} \mathbf{R}^{i\mathrm{T}} \cdot (\hat{\mathbf{s}}^* \hat{\mathbf{s}}^+)\right] \mathrm{d}B \tag{79}$$

Equation (79) is asymmetric with respect to $\mathbf{s}^*$ and $\mathbf{s}^+$ because $\hat{\mathbf{s}}^*\hat{\mathbf{s}}^+ \neq \hat{\mathbf{s}}^+\hat{\mathbf{s}}^*$. The solution algorithm is identical to that of Reference 24. If the configuration is in equilibrium, equation (79) is symmetric.[19,24]

In shell analysis the rotation around the shell normal is usually not considered. Therefore, both formulations coincide, i.e. the tangent stiffness matrix is symmetric in any case. Based on the potential $\Pi[\mathbf{R}(\mathbf{s})\mathbf{a}_3] = \Pi[\bar{\mathbf{a}}_3]$ the stationary condition is

$$\delta\Pi = \int_B \frac{\partial \pi}{\partial \bar{\mathbf{a}}_3} \delta\bar{\mathbf{a}}_3\, \mathrm{d}B = \int_B \frac{\partial \pi}{\partial \bar{\mathbf{a}}_3} \mathbf{a}_3^{\mathrm{T}} \cdot \delta\mathbf{R}\, \mathrm{d}B = \int_B \frac{\partial \pi}{\partial \bar{\mathbf{a}}_3} \bar{\mathbf{a}}_3^{\mathrm{T}} \cdot \mathbf{K}^*\, \mathrm{d}B = \int_B \hat{\mathbf{m}} \cdot \mathbf{K}^*\, \mathrm{d}B = 0 \tag{80}$$

Repeating the arguments used in equations (75) to (77) yields

$$\int_B \frac{\partial \pi}{\partial \bar{\mathbf{a}}_3} \bar{\mathbf{a}}_3^{\mathrm{T}} \cdot \hat{\mathbf{s}}^* \, dB = 0 \tag{81}$$

This equation is again linearized:

$$\int_B \mathrm{D}\left(\frac{\partial \pi}{\partial \bar{\mathbf{a}}_3} \bar{\mathbf{a}}_3^{\mathrm{T}} \cdot \hat{\mathbf{s}}^* \right) dB = \int_B \left[\hat{\mathbf{s}}^{*\mathrm{T}} \cdot \bar{\mathbf{a}}_3 \frac{\partial^2 \pi}{\partial \bar{\mathbf{a}}_3^{\mathrm{T}} \partial \bar{\mathbf{a}}_3} \bar{\mathbf{a}}_3^{\mathrm{T}} \cdot \mathbf{K}^+ + \frac{\partial \pi}{\partial \bar{\mathbf{a}}_3} \bar{\mathbf{a}}_3^{\mathrm{T}} \cdot (\hat{\mathbf{s}}^* \mathbf{K}^+) \right] dB \tag{82}$$

The multiplicative update of the rotations and the subsequent linearization at $\bar{\mathbf{s}} = \mathbf{0}$ leads to

$$\int_B \mathrm{D}\left(\frac{\partial \tilde{\pi}}{\partial \bar{\mathbf{a}}_3} \bar{\mathbf{a}}_3^{i\mathrm{T}} \cdot \hat{\mathbf{s}}^* \right) dB = \int_B \left[\hat{\mathbf{s}}^{*\mathrm{T}} \cdot \bar{\mathbf{a}}_3^i \frac{\partial^2 \tilde{\pi}}{\partial \bar{\mathbf{a}}_3^{\mathrm{T}} \partial \bar{\mathbf{a}}_3} \bar{\mathbf{a}}_3^{i\mathrm{T}} \cdot \hat{\mathbf{s}}^+ + \frac{\partial \tilde{\pi}}{\partial \bar{\mathbf{a}}_3} (\hat{\mathbf{s}}^* \hat{\mathbf{s}}^+ \bar{\mathbf{a}}_3^i) \right] dB \tag{83}$$

Using the relation

$$\hat{\mathbf{s}}^* \hat{\mathbf{s}}^+ = \mathbf{s}^* \otimes \mathbf{s}^+ - (\mathbf{s}^{*\mathrm{T}} \mathbf{s}^+) \mathbf{I} \tag{84}$$

and observing that the incremental rotation vector is orthogonal to the actual director ($\mathbf{s}^{+\mathrm{T}} \bar{\mathbf{a}}_3 = 0$), the term in parentheses in equation (83) is

$$\hat{\mathbf{s}}^* \hat{\mathbf{s}}^+ \bar{\mathbf{a}}_3^i = (\mathbf{s}^* \otimes \mathbf{s}^+ - (\mathbf{s}^{*\mathrm{T}} \mathbf{s}^+) \mathbf{I}) \bar{\mathbf{a}}_3^i = -(\mathbf{s}^{*\mathrm{T}} \mathbf{s}^+) \bar{\mathbf{a}}_3^i = -(\mathbf{s}^{+\mathrm{T}} \mathbf{s}^*) \bar{\mathbf{a}}_3^i \tag{85}$$

It follows that equation (83) is symmetric.

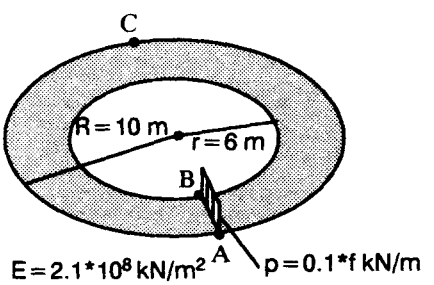

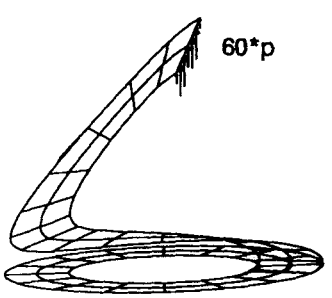

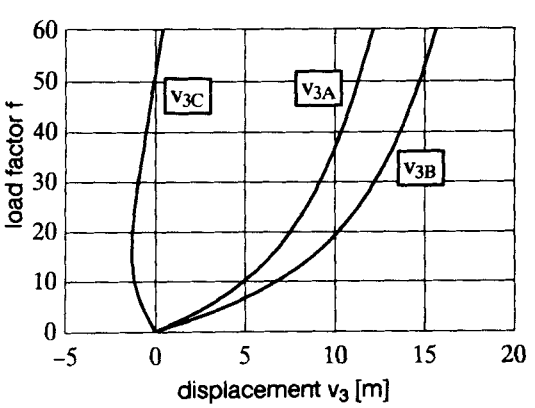

energy norms in
step 3 (f = 4.0 -> f = 6.0)

9.651E+03
6.443E-01
1.608E-02
1.390E-01
5.124E-04
2.493E-03
3.910E-05
4.323E-06
2.005E-07
1.539E-10
4.518E-16

Figure 8. Ring plate

Despite the fact that the update of the rotational parameters in the Newton scheme is not additive, in all numerical examples quadratic convergence could be recognized (see Examples 3.3.1 and 3.3.2).

3.3. Numerical examples

3.3.1. Ring plate loaded at free edge.[4] This example was first presented by Basar and Ding[4] to test finite rotation formulations for shells. The ring plate is loaded at its free edge, the other edge being fully clamped. The load vs displacement diagram (Figure 8) shows the displacement components in the out-of-plane direction of the undeformed plate. The analysis is done using the strains $\hat{\mathbf{E}}_C$ and $\hat{\mathbf{E}}_L$ and a multiplicative update of the rotations. The energy norms for a single load step are given in Figure 8 to show the quadratic convergence for this rotation update.

3.3.2. Pinched hemisphere. This famous benchmark is presented here to show again the quadratic convergence rate for the 'modified' Newton scheme with a non-additive update of the rotations. Here we used 256 four-node assumed strain elements to calculate one quarter of the hemisphere. The interpolation of the shear strains follows the idea of Dvorkin and Bathe. In addition the in-plane shear strains are assumed to be constant. This yields a better element performance for beam-like shell structures. (See Figure 9.)

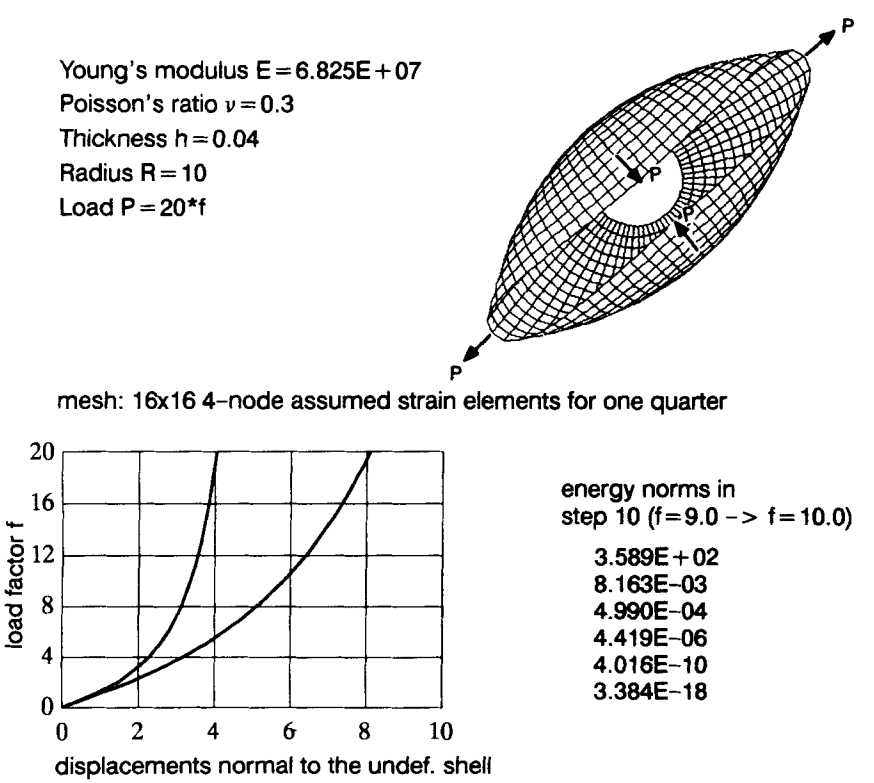

Figure 9. Pinched hemisphere

4. CONCLUSIONS

In order to make special features of degenerated solid and shell theory based elements more transparent an index free (absolute) notation is utilized. This allows that the choice of special co-ordinate systems and discretization schemes do not obscure the mechanical background of the formulation. Their influence can be discussed in a separate step.

The present study refers to a shear flexible 5-parameter shell theory based on a Reissner–Mindlin kinematic, usually applied also in the degenerated solid approach. It allows the following conclusions.

- Numerical integration across the thickness in degenerated solids leads to at least as rigorous elements as their equivalents based on a corresponding shell theory.
- The assumption 'constant Jacobian across the thickness' cause erroneous results for curved elements because rigid body modes are not described in a proper way.
- A series expansion of the inverse Jacobian for the explicit integration across the thickness leads to a shell theory like formulation, but is unnecessary.
- The only difference between 'shell theory' and 'degeneration concept' remains in the kind of discretization.
- In order to avoid too flexible elements for low order elements or coarse meshes, the violation of the assumption 'inextensible shell director' can be circumvented, for example if the components of the rotational vector $\mathbf{s}$ instead of the displacement field $\mathbf{w}$ outside the reference surface are interpolated.

Although it is felt that the recent discussion about the asymmetry or symmetry of the tangent stiffness matrix in large rotation analysis is only of academic interest, the question is again discussed in this paper. Here we use the components of the rotational vector $\mathbf{s}$ as primary variables.

- Starting form a potential a straightforward derivation and linearization with respect to $\mathbf{s}$ leads automatically to a symmetric stiffness matrix.
- Although not necessary, an updated version of the large rotation term may simplify the procedure.
- It is shown how an alternative derivation leads to the asymmetric matrix described in the literature. This can be considered as a consequence of another choice of the test function in the weak formulation.

ACKNOWLEDGEMENTS

The present study is partially supported by a research grant of the German National Science Foundation (DFG) under Ra 218/7–1. This support is gratefully acknowledged.

APPENDIX

1. Additional bending terms in local, orthogonal Cartesian co-ordinates

The local base vectors are denoted by $\mathbf{e}_1, \mathbf{e}_2, \mathbf{e}_3$ and the co-ordinates by y^1, y^2, y^3. $\mathbf{e}_3$ is parallel to $\mathbf{a}_3$.

$$\hat{\beta}_{AB} = \mathbf{e}_A^{\mathrm{T}} \hat{\mathbf{E}}_{\mathrm{L}} \mathbf{e}_B = \beta \tilde{\tilde{\beta}}_{AB} + \frac{1}{2}\left(\frac{\partial \mathbf{v}}{\partial y^A} \frac{\partial \mathbf{a}_3}{\partial y^B} + \frac{\partial \mathbf{a}_3}{\partial y^A} \frac{\partial \mathbf{v}}{\partial y^B} \right) \quad A, B = 1, 2 \tag{86}$$

2. Additional bending terms in global, orthogonal Cartesian co-ordinates

$$\hat{\beta}_{ij} = \mathbf{e}_i^{\mathrm{T}} \hat{\mathbf{E}}_{\mathrm{L}} \mathbf{e}_j = \beta_{ij}^{\sim} + \frac{1}{2}\left(\frac{\partial \mathbf{v}}{\partial x^i} \frac{\partial \mathbf{a}_3}{\partial x^j} + \frac{\partial \mathbf{a}_3}{\partial x^i} \frac{\partial \mathbf{v}}{\partial x^j} + \frac{\partial \mathbf{a}_3}{\partial x^i} \mathbf{w} \frac{\partial \theta^3}{\partial x^j} + \frac{\partial \mathbf{a}_3}{\partial x^j} \mathbf{w} \frac{\partial \theta^3}{\partial x^i} \right) \tag{87}$$

3. Inverse of matrix $\mathbf{T}$

$$\mathbf{T}^{-1}(\mathbf{s}) = \frac{\frac{\phi}{2}}{\tan \frac{\phi}{2}} \mathbf{I} - \frac{1}{2} \hat{\mathbf{s}} + \left(\frac{1}{\phi^2} - \frac{1}{2\phi \tan \frac{\phi}{2}} \right) \mathbf{s} \otimes \mathbf{s} \tag{88}$$

REFERENCES

1. S. Ahmad, B. M. Irons and O. C. Zienkiewicz, 'Curved thick shell and membrane elements with particular reference to axi-symmetric problems', *Proc. 2nd Conf. Matrix Methods in Structural Mechanics*. Wright-Patterson Air Force Base, Ohio, 1968.
2. S. Ahmad, B. M. Irons and O. C. Zienkiewicz, 'Analysis of thick and thin shell structures by curved finite elements', *Int. j. numer. methods eng.*, **2**, 419–451 (1970).
3. Y. Basar and Y. Ding, 'Theory and finite element formulation for shell structures undergoing finite rotations', in G. Z. Voyiadjis and D. Karamanlidis (eds.), *Advances in the Theory of Plates and Shells, Elsevier Science Publishers B.V., Amsterdam*, 1990
4. Y. Basar and Y. Ding, 'Finite-rotation shell elements for the analysis of finite rotation shell problems', Extended abstract of lectures, *Second World Congress on Computational Mechanics*, Aug. 27–31, 1990, Stuttgart, Germany.
5. Y. Basar and W. B. Krätzig, *Mechanik der Flächentragwerke*, Vieweg, Braunschweig, 1985.
6. T. Belytschko, B. L. Wong and H. Stolarski, 'Assumed strain stabilisation procedure for the 9-node Lagrange shell element', *Int. j. numer. methods eng.*, **28**, 385–414 (1989).
7. N. Büchter, 'Ein nichtlineares degeneriertes Balkenelement (2-D) unter Verwendung von Biotspannungen', *Mitteilung Nr. 8*, Instituts für Baustatik, Universität Stuttgart, 1989.
8. A. Cardona and M. Geradin, 'A beam finite element non-linear theory with finite rotations', *Int. j. numer. methods eng.*, **26**, 2403–2438 (1988).
9. M. A. Crisfield, 'Explicit integration and the isoparametric arch and shell elements', *Commun. appl. numer. methods*, **2**, 181–187 (1986).
10. M. Crisfield, 'A consistent co-rotational formulation for non-linear three dimensional beam elements', *Comp. Methods Appl. Mech. Eng.*, to appear.
11. B. M. Irons, 'The semiloof shell element', *Lecture Notes Int. Res. Seminar on Theory and Application of Finite Elements*, University of Calgary, Canada, 1973.
12. R. V. Milford and W. C. Schnobrich, 'Degenerated isoparametric finite elements using explicit integration', *Int. j. numer. methods eng.*, **23**, 133–154 (1986).
13. H. Parisch, 'An investigation of a finite rotation four node assumed strain shell element', *Int. j. numer. methods eng.*, **31**, 127–150 (1991).
14. W. Pietraszkiewicz, 'Geometrically nonlinear theories of thin elastic shells', *Adv. Mech.*, **12**, No. 1 (1989).
15. W. Pietraszkiewicz and J. Badur, 'Finite rotations in the description of continuum deformation', *Int. J. Eng. Sci.*, **21**, 1097–1115 (1983).
16. E. Ramm, 'Geometrisch nichtlineare Elastostatik und finite Elemente', Habilitation, *Bericht Nr. 76-2*, Institut für Baustatik, Universität Stuttgart, 1976.
17. E. Ramm, 'A plate/shell element for large deflections and rotations, *U.S.–Germany Symp. on Formulations and Computational Algorithms in Finite Element Analysis*, MIT, 1976, MIT Press, 1977.
18. E. Reissner, 'On one-dimensional finite-strain beam theory: the plane problem', *ZAMP*, **23**, pp. 795–804 (1972).
19. J. C. Simo, 'The (symmetric) Hessian for geometrically nonlinear models in solid mechanics. Intrinsic definition and geometric interpretation', *Comp. Methods Appl. Mech. Eng.*, to be published.
20. J. C. Simo and D. D. Fox, 'On a stress resultant geometrically exact shell model. Part I: Formulation and optimal parametrization', *Comp. Methods Appl. Mech. Eng.*, **72**, 267–304 (1989).
21. J. C. Simo, D. D. Fox and M. S. Rifai, 'On a stress resultant geometrically exact shell model. Part II: The linear theory', *Comp. Methods Appl. Mech. Eng.*, **73**, 53–62 (1989).
22. J. C. Simo, D. D. Fox and M. S. Rifai, 'On a stress resultant geometrically exact shell model. Part III: Computational aspects of the nonlinear theory', *Comp. Methods Appl. Mech. Eng.*, **79**, 21–70 (1990).
23. J. C. Simo, M. S. Rifai and D. D. Fox, 'On a stress resultant geometrically exact shell model. Part IV: Variable thickness shells with through-the-thickness stretching', *Comp. Methods Appl. Mech. Eng.*, **81**, 53–91 (1990).

24. J. C. Simo and L. Vu-Quoc, 'On the dynamics of 3-d finite-strain rods', *Finite Element Methods for Plate and Shell Structures, 2: Formulations and Algorithms*, Pineridge Press, Swansea, U.K., 1986, pp. 1–30.
25. N. Stander, M. Matzenmiller and E. Ramm, 'An assessment of assumed strain methods in finite rotation shell analysis', *Eng. Computations*, **6**, 57–66 (1989).
26. G. M. Stanley, 'Continuum-based shell elements', *Ph.D. Thesis*, Stanford University, 1985.
27. G. M. Stanley, K. C. Park and T. J. R. Hughes, 'Continuum-based resultant shell elements', in T. J. R. Hughes *et al.* (eds.), *Finite Element Methods for Plate and Shell Structures*, Pineridge Press, Swansea, U.K., 1986, pp. 1–45.
28. O. C. Zienkiewicz, R. L. Taylor and J. M. Too, 'Reduced integration technique in general analysis of plates and shells', *Int. j. numer. methods eng.*, **3**, 275–290 (1971).